

Marquette University

e-Publications@Marquette

Chemistry Faculty Research and Publications

Chemistry, Department of

7-2022

UV- and Visible-Light Photopatterning of Molecular Gradients Using the Thiol–yne Click Reaction

Mark Mitmoen

Marquette University, mark.mitmoen@marquette.edu

Ofer Kedem

Marquette University, ofer.kedem@marquette.edu

Follow this and additional works at: https://epublications.marquette.edu/chem_fac

 Part of the [Chemistry Commons](#)

Recommended Citation

Mitmoen, Mark and Kedem, Ofer, "UV- and Visible-Light Photopatterning of Molecular Gradients Using the Thiol–yne Click Reaction" (2022). *Chemistry Faculty Research and Publications*. 1061.

https://epublications.marquette.edu/chem_fac/1061

Marquette University

e-Publications@Marquette

Chemistry Faculty Research and Publications/College of Arts and Sciences

This paper is NOT THE PUBLISHED VERSION.

Access the published version via the link in the citation below.

ACS Applied Materials & Interfaces, Vol. 14, No. 28 (July 2022): 32696-32705. [DOI](#). This article is © American Chemical Society and permission has been granted for this version to appear in [e-Publications@Marquette](#). American Chemical Society does not grant permission for this article to be further copied/distributed or hosted elsewhere without express permission from American Chemical Society.

UV- and Visible-Light Photopatterning of Molecular Gradients Using the Thiol–yne Click Reaction

Mark Mitmoen

Department of Chemistry, Marquette University, Milwaukee, Wisconsin

Ofer Kedem

Department of Chemistry, Marquette University, Milwaukee, Wisconsin

Abstract

The rational design of chemical coatings is used to control surface interactions with small molecules, biomolecules, nanoparticles, and liquids as well as optical and other properties. Specifically, micropatterned surface coatings have been used in a wide variety of applications, including biosensing, cell growth assays, multiplexed biomolecule interaction arrays, and responsive surfaces. Here, a maskless photopatterning process is studied, using the photocatalyzed thiol–yne “click” reaction to create both binary and gradient patterns on thiolated surfaces. Nearly defect-free patterns are produced by first coating glass surfaces with mercaptopropylsilatrane, a silanizing agent that forms smoother self-assembled monolayers than the commonly used 3-mercaptopropyltrimethoxysilane.

Photopatterning is then performed using UV (365 nm) or visible (405 nm) light to graft molecules onto the surface in tunable concentrations based on the local exposure. The technique is demonstrated for multiple types of molecular grafts, including fluorescent dyes, poly(ethylene glycol), and biotin, the latter allowing subsequent deposition of biomolecules via biotin–avidin binding. Patterning is demonstrated in water and dimethylformamide, and the process is repeated to combine molecules soluble in different phases. The combination of arbitrary gradient formation, broad applicability, a low defect rate, and fast prototyping thanks to the maskless nature of the process creates a particularly powerful technique for molecular surface patterning that could be used for a wide variety of micropatterned applications.

KEYWORDS:

Silanization, photopatterning, surface patterning, thiol–yne reaction, click chemistry, molecular gradients

1. Introduction

The precise and selective deposition of molecules on substrates, known as molecular printing, has developed extensively in recent years.^(1–6) Modifying the chemical properties of surfaces tunes their interactions with molecules and nano- and microscale objects,^(7,8) including cells.^(9,10) Patterned surfaces are of particular importance in biological applications such as biosensors,^(3,11–15) bioelectronics,^(16,17) and cell growth assays.^(2,9,18) Molecular printing also enables the generation of multiplexed arrays to explore the behavior of cells and biomolecules in a wide variety of microenvironments.⁽⁶⁾ Surface gradients, such as of hydrophobicity or the concentration of specific binding sites, are used to study cell adhesion and migration.^(19,20) Surface gradients also allow for the transport of droplets via a ratchet mechanism^(21,22) and the generation of solvent flows in microfluidic systems.⁽²³⁾ The accelerating development of responsive surfaces and surface-based chemical reactions will particularly benefit from a robust gradient patterning ability.^(24,25)

There are a wide variety of molecular printing techniques combining various elements in creative ways, so it is difficult to categorize them. One common category is direct write methods, such as direct laser writing,⁽²⁶⁾ droplet spotting,^(4,27) and dip-pen nanolithography,^(28,29) which offer high resolution but slow rates; the rate limitation is partially alleviated by the use of polymer pen lithography, where arrays containing up to millions of individual tips simultaneously generate identical patterns.⁽²⁹⁾ Tip arrays have also been used for photopatterning, where tips with small apertures⁽³⁰⁾ or even aperture-less tips⁽³¹⁾ serve as near-field probes to produce arrays of subwavelength features.⁽²⁹⁾ More recently, beam pen arrays were used to photochemically generate patterns of polymer brushes, creating 3D structures.^(6,32,33)

The other major category is of parallel methods such as microcontact printing⁽³⁴⁾ and mask-based photolithography,^(10,26,35–38) both of which allow fast replication but require the time-consuming and expensive production of a master stamp or mask and do not allow for the creation of complex gradients. Maskless photolithography, which uses computerized image projection systems, is quickly becoming a highly capable technique in the molecular printing field.⁽³⁹⁾ Notably, maskless photopatterning has been demonstrated for proteins, relying on their ability to bind nonspecifically to deprotected surfaces,⁽⁴⁰⁾ and for creating complex 3D polymer structures.⁽⁴¹⁾ To enable the specific binding of a wide range of molecules, a particularly promising tool is the photocatalyzed thiol–ene/yne click reaction,⁽⁴²⁾ as alkyne functionalities are commonly added to biomolecules and other functional

materials. The specificity to terminal alkenes and alkynes means that the reaction is considered to be bio-orthogonal.⁽²⁶⁾ Thiol-ene/yne reactions have been demonstrated with mask-based photopatterning,^(26,35,43–45) beam pen lithography,⁽³²⁾ or microcontact printing^(46,47) to deposit a variety of molecules in binary (monochrome) patterns, confirming their broad applicability. The quality of the obtained patterns was limited, however, by the surface-modification agent employed. Flaws in patterns result in unpredictable surface concentrations, which restrict the applicability of the surface for quantitative applications and limit the performance of functional surfaces.

Here, we demonstrate a general technique for photopatterning surfaces with molecular gradients of arbitrary molecules, producing high-quality patterns using maskless photolithography for fast and easy prototyping. Patterning is based on the thiol-yne click reaction, which is widely applicable for biomolecules, with easily obtained reagents and standardized alkylation procedures. To obtain high-quality patterns, we utilize a recently developed surface modification agent, mercaptopropylsilatrane (MPS).⁽⁴⁸⁾ MPS has been shown to produce a smoother surface with fewer defects compared to the commonly used 3-mercaptopropyltrimethoxysilane (MPTMS; see structures in Figure 1A) and is less prone to spurious polymerization.⁽⁴⁸⁾ We use a digital micromirror device (DMD) to project patterns of UV (365 nm) or visible (405 nm) light and to control the exposure at each pixel individually, enabling fine control over the concentration of patterned molecules. The use of visible light is crucial for the deposition of UV-sensitive biomolecules. Each pattern is deposited in minutes, and the technique is demonstrated for molecules soluble in water or dimethylformamide (DMF), even deposited subsequently on the same sample. This powerful, additive photopatterning technique expands the capability to produce accurate patterns of finely controlled densities and will support the studies of biomolecule interactions, responsive surfaces, and surface-based reactions.

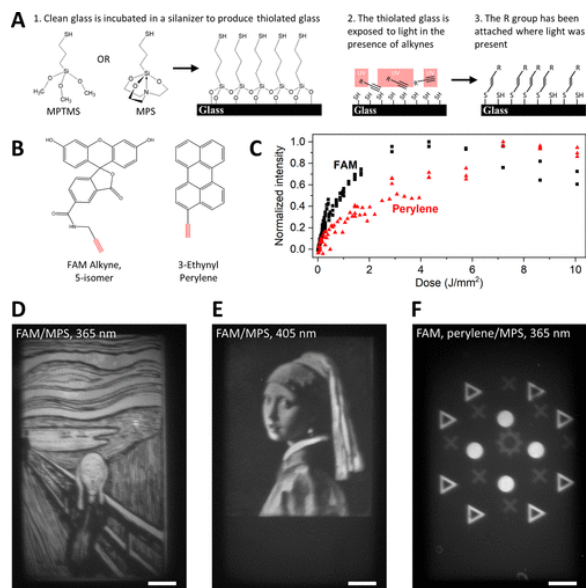


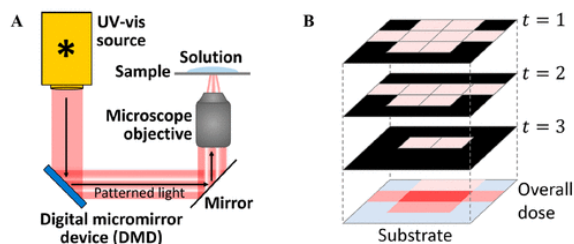
Figure 1. (A) Overview of the synthetic procedure. (B) Chemical structures of the two dyes. (C) Fluorescence intensity above the background vs the 365 nm dose on MPTMS, normalized to the highest intensity of each dye. (D–F) Fluorescent images of (D) a monochrome pattern of FAM in the shape of the lithograph version of *The Scream* by Edvard Munch, patterned with 365 nm light. (E) Gradient pattern of FAM in the shape of *Girl with a Pearl Earring* by Johannes Vermeer, patterned with 405 nm light. (F) Monochrome patterns of FAM and perylene dyes in the same field of view, where the brighter pattern is

FAM and the dimmer is perylene. Panels D–F were patterned on MPS and imaged dry. Scale bars represent 100 μm .

2. Results and Discussion

2.1. Photopatterning Process

We developed and applied the photopatterning process for four species, demonstrating the broad applicability of this method: (i) the fluorescent dye 3-ethynyl perylene (henceforth called “perylene”) in the organic solvent DMF; (ii) the fluorescent dye FAM alkyne, 5-isomer (“FAM”, a fluorescein derivative) in water; (iii) biotin-PEG₄-alkyne (“biotin”) in water, to which we then bind the protein avidin, labeled with fluorescein; and (iv) methoxy poly(ethylene glycol)-alkyne 5 kDa (“PEG”) in water. We photopatterned with 365 nm light using the radical photoinitiator 2-hydroxy-4'-(2-hydroxyethoxy)-2-methylpropiophenone and with 405 nm light using the radical photoinitiator lithium phenyl-2,4,6-trimethylbenzoylphosphinate. The photopatterning system includes three main parts: (i) a light source, consisting of a 48 W, 365 nm LED or a 50 W, 405 nm LED; (ii) a computer-controlled pattern projector, based on a digital micromirror device (DMD); and (iii) an inverted fluorescence microscope. Light travels through a liquid light guide from the LEDs to the pattern projector, and the light pattern is then focused by the microscope objective onto the substrate, which is coated with several drops of photopatterning solution. A simplified diagram of the experimental setup is shown in Scheme 1A. The chemical process is provided in Figure 1A, and the structure of the fluorescent dyes is shown in Figure 1B; note that the patterned molecule may bind to two sulfur groups on the surface. To form monochrome patterns, where each pixel is either exposed, and therefore coated with molecules, or is not, we projected a static image onto the glass substrate for the desired duration. To produce grayscale patterns, where the surface density of the patterned monolayer was individually controlled at each pixel, we first selected a desired range of doses based on dose–response tests (Figure 1C). We then processed a grayscale image to assign a desired exposure time for each pixel. (The computer script for generating image sequences is provided as Supporting Information.) We then projected a series of images (stack) onto the substrate, and in each image, different pixels were illuminated such that the overall light dose was individually controlled per pixel (Scheme 1B). The image stack was corrected for a vignetting effect in our optical setup (the dose decreases from the center of the projected image toward the edges) so that each pixel receives the intended UV dose (see the Supporting Information). This control allows us to form complex gradients of monolayer density.



Scheme 1. (A) Simplified Schematic of the Experimental Setup and (B) Formation of Grayscale Patterns^a
^aLight is directed toward a DMD, focused through the objective of an inverted fluorescence microscope, and focused onto the top surface of a glass slide coated with a photopatterning solution. To form grayscale patterns, a series of monochrome images are projected such that the total dose at each pixel is finely controlled.

2.2. Preparation of Thiolated Substrates

Our patterning method relies on reactions between thiols and terminal alkynes. We chose to locate the thiols on the surface because functionalizing molecules with alkynes is somewhat easier than with thiols, and a wide range of alkyne-terminated molecules are available commercially.⁽⁴⁹⁾ To produce a thiolated surface, cleaned glass coverslips (henceforth referred to as “slides”) were silanized with either MPTMS or MPS; we synthesized MPS following a literature procedure.⁽⁴⁸⁾ MPTMS was deposited following a common literature procedure, and we optimized the deposition of MPS. The thiolated surface is more hydrophobic than the clean glass, so the extent and reproducibility of the deposition were evaluated using the advancing water contact angle (WCA) method and also by the quality of the subsequent photopatterning for samples possessing the expected WCAs. A full list of experimental conditions and resulting WCAs can be found in Table S1 in the Supporting Information, and the optimal conditions used for the images presented here are listed in the Experimental Section. WCA values (means and standard deviations of eight samples each, three points per sample) were $61.0 \pm 2.2^\circ$ for MPTMS and $50.2 \pm 2.3^\circ$ for MPS, within the expected 50–70° range reported in the literature for full thiol monolayers.^(50–52)

2.3. Photopatterning Produces Both Monochrome and Grayscale Images

We first demonstrate the generation of a monochrome pattern, Figure 1D, a black and white version of Edvard Munch’s *The Scream*, which we exposed for 3 min (365 nm, 430 mJ/mm² at the center of the image; the dose decreases toward the edges because of a vignetting effect in the optical setup) using FAM on an MPS-coated substrate. The resulting fluorescent image demonstrates the sharpness and high contrast achievable with this technique. The smallest features visible in the image (e.g., the vertical lines to the right of the person) are approximately 5 μm wide. The image was produced and imaged using a 10× objective, for which the projected pixels from the DMD would be approximately 0.7 μm wide (per the specifications). Factors limiting the resolution include scattering at several interfaces and the diffusion of excited photoinitiator radicals and/or dye molecules. We patterned images of similar quality using perylene (Figures S3 and S4). For FAM, PEG, and biotin deposition, a photoinitiator was included in the photopatterning solution to absorb the UV or visible light and produce a radical. Curiously, we found that no photoinitiator was needed to pattern perylene. It has been shown in the literature that at least some dyes form radicals upon irradiation and catalyze bond formation, a process typically used for proteins and termed “protein adsorption by photobleaching” (PAP).⁽³⁹⁾ We speculate that this is the cause of our experimental results due to perylene’s relatively strong absorption at 365 nm (Figure S5).

To generate grayscale (variable density) patterns, we determined the relationship between exposure time and the extent of deposition. We projected a standard test pattern (Figure S8) onto the slide for different durations with 365 nm light, for both perylene and FAM, and then quantified the resulting fluorescence intensity, which acts as a proxy for the concentration of dye at the surface (Figure 1C). There is a steady but nonlinear increase in fluorescence intensity with an increase in exposure time up to a dose of approximately 4.0 J/mm² (at around 30 min of exposure); longer exposures led to a decrease in fluorescence intensity. During the long exposure, it is likely that the UV light degrades some already-attached dye molecules at a rate exceeding additional attachment at high surface coverage. Additionally, it is possible that self-quenching, known to occur for fluorescein-based dyes at high concentrations, is involved, consistent with the fact that the decrease is more prominent for FAM.⁽⁵³⁾ As a compromise between the patterning time and the resulting intensity, we chose to use doses in the hundreds of mJ/mm² (durations of a few minutes) for most patterns in this study. Conveniently, the intensity–dose curve in this region was approximately linear (Figure S9), making it easier to design

gradients. A gradient pattern (*Girl with a Pearl Earring* by Johannes Vermeer) is shown in Figure 1E, patterned using 405 nm light with a maximum dose of 455 mJ/mm², with FAM on an MPS-coated substrate; the exposure took a little over a minute. The image displays a range of fluorescence intensities, indicating different monolayer densities. Additional images produced using different dyes, surfaces, and irradiation wavelengths are provided in the Supporting Information, Figures S3, S4, and S10–S12.

2.4. A Surface Can Be Patterned More Than Once to Deposit Different Molecules

An important goal in photopatterning is to combine multiple molecules on the same substrate. This requires the first patterning step and subsequent cleaning to avoid damaging any unexposed areas so that they remain receptive to further depositions. Similarly, the second deposition process and subsequent cleaning must not damage the previously deposited dye. Figure 1F shows a pattern composed of the two dyes. The order of deposition of the two dyes makes no difference to the final image, proving neither step significantly damages the attached dyes or the exposed thiol surface. This result demonstrates the robustness of the sulfur–carbon bond formed in the patterning as well as that of the thiol monolayer on the glass surface.

2.5. MPS Provides Higher-Quality Patterns and Is More Resistant to DMF but Produces Lower Dye Densities Compared to MPTMS

In this study, we used two silanizing agents—the commonly used MPTMS and the more recently developed MPS. The latter has been shown to produce smoother films and is less prone to polymerization, which is common for MPTMS depositions.⁽⁴⁸⁾ Figure 2 provides representative images of perylene and FAM on the two coatings (see additional images in the Supporting Information). When using MPTMS (Figure 2A,C), we observed two types of defects—dark spots, likely holes in the film, and bright spots, which we interpret as polymerization of the MPTMS, which provides a large number of thiol groups available to bind to the fluorescent dye. Deposition of the DMF-soluble dye perylene, which is followed by sonication in DMF, appears to be especially damaging to the MPTMS film. When patterning the same dyes on MPS (Figure 2B,D,E), we observed far fewer defects of both types; the small bright spots in Figure 2B are likely the result of dye aggregation, as we have observed previously, rather than coating defects. However, the MPS images display a lower intensity; for similar UV doses, the MPTMS film provided 6-fold the fluorescence intensity (Figure 2F). This result implies that while MPS likely forms a smoother and more robust film, MPTMS provides a higher density of available thiol binding sites, which may simply be the result of MPTMS forming multiple layers rather than a monolayer. When the same pattern is deposited with FAM on MPS using 405 nm light (Figure 2E), particularly good contrast and detail are achieved.

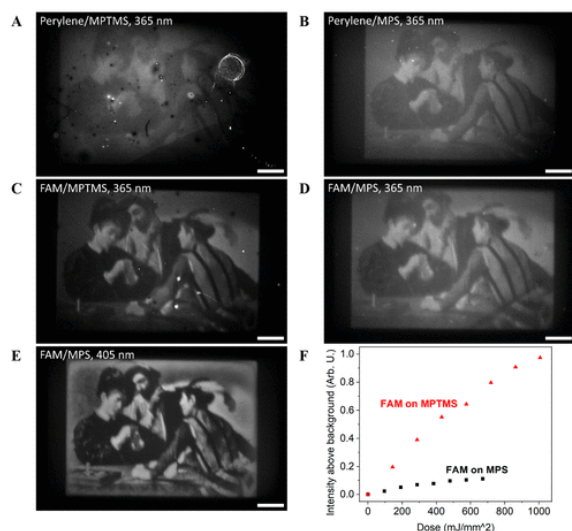


Figure 2. (A–D) Photopattern in the shape of *The Cardsharps* by Caravaggio demonstrating the comparison between the silanization agents MPTMS and MPS for the two dyes, perylene and FAM, patterned using 365 nm light. Panel C was patterned with one-third the maximal dose of panel D and imaged under lower power (30 vs 100%). (E) The same pattern, deposited with FAM on MPS using 405 nm light. (F) Intensity above the background level of test patterns of FAM on MPTMS and MPS using 365 nm light. All patterns were imaged in air; images were shaded differently to account for varying intensities between dyes and coatings. Scale bars represent 100 μm .

2.6. Patterning of Biotin-PEG₄-Alkyne Allows Immobilization of the Avidin Protein

The binding between biotin and the protein avidin (or the related streptavidin) is one of the strongest known noncovalent interactions⁽⁵⁴⁾ and is very commonly used for bioconjugation, as biotin groups are readily and routinely added to biomolecules. Each avidin protein can bind four biotin groups and so is often used in a sandwich configuration, with an avidin connecting two or more biotinylated species. Indeed, biotin–avidin chemistry has often been used in the surface patterning of biomolecules.^(26,35,39,55–57) We photopatterned biotin-PEG₄-alkyne and then incubated the slide in a solution of fluorescein-labeled avidin (Figure 3A). We observe a clear fluorescent image in the shape of the pattern used for biotin deposition, indicating successful biotin patterning (Figure 3B); the image shows typical MPTMS defects. This pattern of avidin may later be used to bind biotinylated biomolecules, as amply demonstrated in the literature.^(26,35) Using a sandwich configuration means that the immobilized molecules, aside from the initial alkyne-biotin layer, are never exposed to the strong patterning light, which may damage their function.

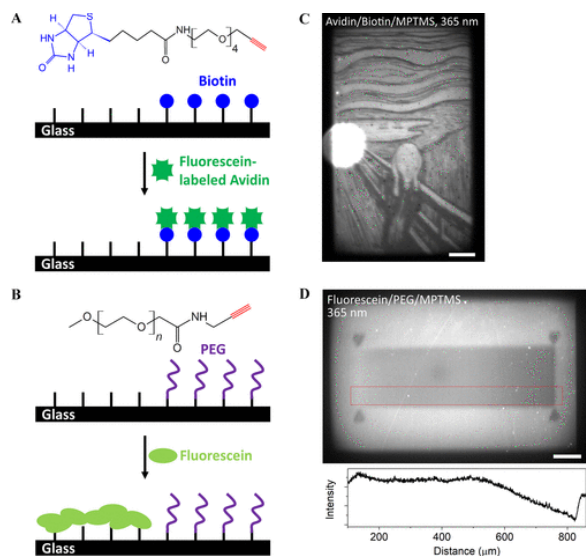


Figure 3. (A) Structure of biotin-PEG₄-alkyne, with biotin in blue and alkyne in red, and scheme of biotin-avidin patterning. (B) Fluorescence microscopy image of the patterned fluorescently labeled avidin. (C) Structure of PEG-alkyne (mean molecular weight 5 kDa), with alkyne in red, and scheme of PEG surface protection. (D) Fluorescence microscopy image and intensity profile (of the region marked with the red box) of the PEG-protected surface (gradient with a maximum dose of 4 J/mm² at the right edge of the image) after incubation in fluorescein. Scale bars represent 100 μm.

2.7. Patterned Poly(ethylene glycol) Reduces Nonspecific Adsorption

When patterning surfaces, we may wish not only to deposit molecules but in some cases to prevent their deposition in selected regions. Surfaces are often protected from nonspecific binding using poly(ethylene glycol).^(9,40) We patterned a gradient of alkyne-terminated poly(ethylene glycol) (5 kDa mean molecular weight) and then incubated the slide in a solution of fluorescein followed only by rinsing, without lengthy incubation or sonication (Figure 3C). The resulting image (Figure 3D) shows a strong contrast between the patterned region (dark gradient) and the background and thus demonstrates the ability of PEG to reduce nonspecific binding.

2.8. Patterned FAM Alkynes Act as a pH Sensor

The intensity of fluorescence emission from fluorescein and its derivatives is known to vary on the basis of solution pH, with acidic conditions nearly quenching the emission.⁽⁵⁸⁾ We envision using a patterned patch of FAM to report on the local pH, which might be affected by a reaction occurring at the surface, which is an application previously demonstrated using microcontact printing.⁽⁵⁹⁾ We imaged the same pattern under the same conditions, changing only the pH of the buffer with which the patterned substrate was wetted, ranging from a pH of 3.87 to 10.19 (Figure 4A–D). The patterned FAM (a fluorescein derivative) still responds to pH, despite immobilization, interaction with adjacent dye molecules, and exposure to strong UV light during deposition. To quantify the response, we also imaged a standard exposure pattern (Figure S8), and the results are shown in Figure 4E. The different FAM surface concentrations, resulting from different patterning doses, all respond similarly to the pH. This result demonstrates that interactions between the FAM and the surface and between nearby FAM molecules do not impair FAM's ability to sense and report on pH.

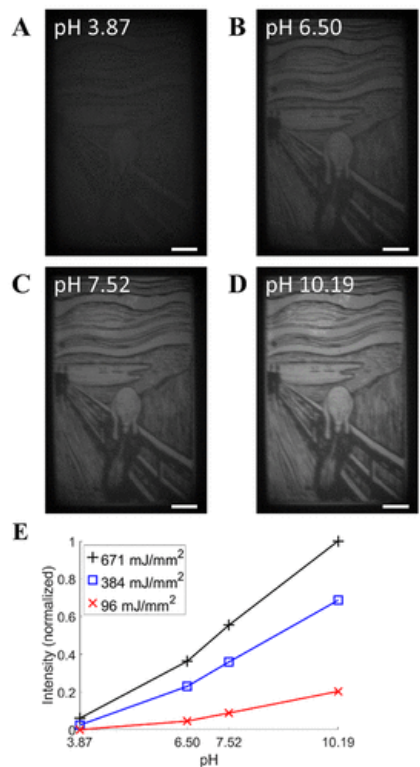


Figure 4. (A–D) The same pattern (FAM/MPS, 365 nm) imaged under different buffer solutions: (A) citrate, pH 3.87; (B) phosphate, pH 6.50; (C) PBS, pH 7.52; and (D) carbonate, pH 10.19. (E) Comparison of intensity from an exposure test (Figure S8) imaged in the same buffers. The order of evaluation was citrate, carbonate, phosphate, and then PBS to verify that the loss in emission intensity was primarily due to the change in pH rather than bleaching. See Figure S13 for observed bleaching as a result of repeated imaging of the sample. Scale bars represent 100 μm .

3. Conclusions

The ability to localize molecules on surfaces is highly valuable to multiple fields and enables progress toward capable surface-based devices. In this study we developed, for the first time, the ability to use the thiol–yne click reaction to create complex gradient patterns of a variety of alkynated molecules. The alkylation of biomolecules is a common and straightforward procedure, making this a widely applicable method. Even more ubiquitous is the biotinylation of molecules for biotin–avidin binding, so we demonstrated the deposition of biotin, which, when coated with avidin, enables the attachment of biotinylated species. The use of visible light further assists the deposition of biomolecules, which tend to be sensitive to UV light, and will particularly help sequential deposition in the same or nearby regions. Using the biotin–avidin route will allow the deposition of biotinylated molecules without ever exposing them to strong light. The deposition of a PEG layer demonstrates selective protection of the surface from nonspecific attachment. Our maskless process using a DMD eliminates the need to produce costly masks or stamps and enables per-pixel dose control to produce gradients. Our use of the recently developed silanizing agent MPS resulted in high-quality patterns, greatly improving upon previous demonstrations. We have demonstrated the reusability of the surface and the robustness of the thiol film by subsequently depositing two dyes in the same pattern. Materials localized on the surface need to be functional, and we verified that our deposited FAM maintains its well-known and reversible sensitivity to pH; a patch of FAM monolayer is therefore able to act as a reporter for local pH. Overall,

we have developed a flexible approach for depositing a wide range of molecules in high-quality patterns with finely controlled surface concentrations. We expect that this approach will enable the development of capable and innovative devices based on functional monolayers.

4. Experimental Section

4.1. Materials

Microscope cover glasses (22 × 22 mm²), no. 2 thickness (VWR) and no. 4 thickness (ORSAtec). Solvents: chloroform (HPLC grade, J.T. Baker); dichloromethane (“DCM”, ACS, VWR); dimethyl sulfoxide (“DMSO”, ACS, J.T. Baker); dimethylformamide (“DMF”, ACS, Macron Fine Chemicals); sulfuric acid (Macron Fine Chemicals); hydrogen peroxide 30% (Baker Analyzed, J.T. Baker); methanol (ACS, Fisher Scientific); *n*-pentane (HPLC grade, Alfa Aesar); reagent alcohol, absolute (Macron Fine Chemicals); and toluene (ACS, Macron Fine Chemicals). Salts: citric acid monohydrate (ACS, Alfa Aesar); PBS buffer tablets that each produce 100 mL of 10 mM solution (VWR); potassium carbonate (Baker Analyzed, J.T. Baker); potassium hydrogen phosphate, dried (98+%, Alfa Aesar); potassium phosphate, monobasic (ACS, LabChem); sodium bicarbonate (ACS, Macron Fine Chemicals); sodium carbonate (ACS, LabChem); sodium citrate (USP, Sigma); sodium dodecyl sulfate (Baker Analyzed, 95%, J.T. Baker); and sodium hydroxide (Acros Organics). Surface modification and patterning: biotin-PEG4-alkyne (“biotin”, Broadpharm); 3-ethynyl perylene dye (“perylene”, Lumiprobe); FAM alkyne, 5-isomer dye (“FAM”, Lumiprobe); fluorescein disodium salt hydrate (Beantown Chemical); Fluorescein Avidin D (Vector Laboratories); 2-hydroxy-4'-(2-hydroxyethoxy)-2-methylpropiophenone (“UV photoinitiator”, TCI); lithium phenyl (2,4,6-trimethylbenzoyl) phosphinate (“visible photoinitiator”, TCI America); 3-mercaptopropyltrimethoxysilane (“MPTMS”, 95%, TCI); methoxy poly(ethylene glycol)-alkyne, 5 kDa (“PEG”, Nanosoft Polymers); and triethanolamine (98+%, Alfa Aesar). All materials were used as received. Milli-Q water was produced in-house. Stock solution vials (of the deposition molecules, photoinitiators, or MPS) were covered in aluminum foil and stored at 4 °C.

4.2. Methods

4.2.1. Synthesis of MPS

Mercaptopropylsilatrane (MPS) was synthesized⁽⁴⁸⁾ and purified^(48,60) on the basis of literature procedures. In-depth procedures are provided in the Supporting Information. The MPS product had the following proton NMR data (see Figure S14): ¹H NMR (400 MHz, DMSO) δ 4.33 (t, *J* = 5.6 Hz, 1H), 3.57 (t, *J* = 5.9 Hz, 6H), 2.75 (t, *J* = 5.9 Hz, 6H), 2.52 (t, *J* = 6.1 Hz, 2H), 2.33 (q, *J* = 7.5 Hz, 2H), 1.97 (t, *J* = 7.7 Hz, 1H), 1.51 (p, *J* = 7.7 Hz, 2H), 0.24–0.15 (m, 2H).

4.2.2. Substrate Preparation and Cleaning

Microscope cover glasses were cut into two separate 9 mm × 22 mm pieces using a diamond scribe. The glass coverslip halves (slides) were then numbered and marked with a diamond scribe to aid in orienting and focusing on the slide. A PTFE holder with prepared slides was submerged in a freshly prepared piranha solution consisting of a 3:1 ratio of sulfuric acid to 30% hydrogen peroxide. (**Caution!** Piranha solution is extremely corrosive and boils upon mixing. It continues to outgas for days and so should be kept in an open or vented container before neutralization or disposal.) After a 1 h treatment, the holder was removed from the piranha solution and the solution was removed and placed in a waste container. The holder was subsequently placed back into the cleaned, empty jar, and the holder, glass slides, and jar were washed three times with Milli-Q water and three times with methanol. If the slides were to be

silanized with MPS, then they were dried with a stream of N₂. If the slides were to be silanized with MPTMS, then they were also rinsed three times with toluene.

4.2.3. MPTMS Silanization

The slides in the holder were then lowered into a 1% v/v solution of MPTMS in toluene to submerge the slides in the silanization solution. The jar was then purged with N₂ and sealed. The slides were incubated in the silanization solution for 2 h. The slides were then rinsed three times with toluene, three times with methanol, and dried under an N₂ stream. While trace amounts of water are necessary for the silanization process, excess water will result in polymerization, which appears as white solids on the slide. To alleviate this problem, a fresh bottle of toluene, or dry toluene, may be used. A very wide range of deposition conditions are found in the literature in terms of solvent, concentration, duration, and more, and we did not extensively optimize this step.

4.2.4. MPS Silanization

We explored a variety of procedures, listed in the Supporting Information section. Following an optimization process, the patterns shown in this article result from one of two procedures, which produce similar results: (1) Shell vials were prepared with 2.925 mL of toluene and 0.075 mL of 200 mM MPS in DMSO (final concentration of 5 mM), and the vial was capped and vortex mixed for 10 s. The slide was added, the air above the solution was gently purged with N₂, and the vial was capped for a 24-h incubation. Following incubation, the slides were inserted into a PTFE holder, and the entire holder and slides were rinsed three times in ethanol by submerging the holder in a fresh beaker of ethanol. After drying under an N₂ stream, the slides were cured at 80 °C for 1 h;⁽⁴⁸⁾ the curing step promotes the formation of Si–O–Si bonds by condensation, which likely increases stability via cross-linking of the silanes.^(48,61) The slides were removed from the oven and allowed to cool to room temperature on the counter. A more gradual cooling step was found to decrease the final image quality. The hydrophobicity of the slides was measured using the advancing water contact angle method with an Ossila contact angle goniometer. (2) Alternatively, the cleaned glass slides were treated for 20 min with an Ossila UV ozone cleaner (an oxygen plasma treatment was previously found to assist silanization⁽⁴⁸⁾). The slides were placed in a PTFE holder and then into a jar containing a 5 mM solution of MPS in ethanol. The jar was covered with aluminum foil and heated to 60 °C. The slides were incubated for a total of 4.5 h, following which the slides were rinsed three times with ethanol and dried with an N₂ stream. The advancing WCA result for an average of four slides, with three spots measured on each, was 48 ± 1°; when the UV ozone treatment was omitted, the average was 37 ± 12°, indicating a nonuniform and incomplete coating. The slides were not further cured. The second procedure was found to be more reliable and less prone to polymerization or a nondeposition (indicated by hydrophilic WCAs), which did occur occasionally with the first procedure.

4.2.5. Photopatterning

A single glass slide was placed in a glass-bottomed Petri dish (WillCo Wells) and placed above the objective on a movable stage of an Olympus IX81 fluorescence microscope with a Mightex Polygon 1000-G system (1300 pixels × 800 pixels, 7.6 μm pixel size) and a 10×/0.30 UPlanFL N objective. Different high-power LEDs (Mightex; 365 nm, 48 W; 405 nm, 50 W; 455 nm, 3 W; and 505 nm, 12 W) are combined with a series of beam combiners and connected to the Polygon unit via a liquid light guide. Micro-Manager software⁽⁶²⁾ was used to set the x–y–z coordinates of planned photopatterning locations on the top surface of the slide. The slide was covered with a few drops of the photopatterning solution,

and a cover was put on the glass Petri dish to reduce evaporation. The previously set stage coordinates were used to move the stage so that the patterned beam of light would be in focus when projected onto the surface of the slide. The Polygon and the LEDs were coordinated and triggered using a TTL signal train generated by a Pulser unit (Prizmatix). UV-vis absorbance spectra (collected using a Jasco V-570 spectrophotometer) for 3-ethynyl perylene and FAM alkyne, 5-isomer are provided in Figure S5, and fluorescence emission and excitation spectra (collected using a Photon Technology Fluorimeter) are provided in Figures S6 and S7, respectively.

For patterning 3-ethynyl perylene, 3 drops of a 2 mM solution in DMF were used. Following exposure, the slides were sequentially rinsed with methanol and DMF to remove the dye solution, followed by three sonication steps of 10 min each in DMF. The slides were then rinsed three times with methanol and dried with an N₂ stream.

For patterning FAM alkyne, 5-isomer, 100 μ L of a 1:1 ratio of 0.2 mM solution of the dye to 4 mg/mL photoinitiator (either the UV or visible-light photoinitiator) in a 10 mM carbonate buffer at a pH of 10.19 was used (final concentrations of 0.1 mM and 2 mg/mL, respectively). Following exposure, the slides were rinsed with ethanol and then sonicated three times for 10 min each in ethanol. After a final rinse with ethanol, the slides were dried with an N₂ stream.

For patterning biotin-PEG₄-alkyne, a 10 mM solution was prepared in Milli-Q water and filtered through a 0.22 μ m PTFE syringe filter. The photopatterning solution was 100 μ L of a 1:1 ratio of 10 mM biotin-PEG₄-alkyne to 4 mg/mL UV photoinitiator (final concentrations of 5 mM and 2 mg/mL, respectively). After photopatterning, the slide was rinsed with Milli-Q water before two sonications in Milli-Q water for 15 min each. The slide was rinsed in buffer (in this paragraph, "buffer" refers to 1 \times PBS buffer with 0.5 mg/mL sodium dodecyl sulfate, adjusted to a pH of 8.20) before incubating in a 100 nM solution of fluorescein avidin D in buffer for 15 min. After rinsing with fresh buffer twice, the slide was stored in fresh buffer in a shell vial overnight at 4 $^{\circ}$ C. The slide was then incubated in fresh buffer at room temperature for 4.5 h and then again for an additional 3 h. After a final rinse in buffer, the slide was rinsed three times with Milli-Q water before drying with an N₂ stream, following which the slide was imaged. Note that the incubation durations were chosen arbitrarily and were not optimized.

For patterning methoxy poly(ethylene glycol)-alkyne 5 kDa (PEG-alkyne), a 10 mg/mL solution was prepared in Milli-Q water and filtered through a 0.22 μ m PTFE syringe filter. The photopatterning solution was 100 μ L of a 1:1 ratio of 10 mg/mL PEG-alkyne to 4 mg/mL UV photoinitiator (final concentrations of 5 and 2 mg/mL, respectively). After photopatterning, the slide was sonicated in ethanol three times for 10 min each, followed by drying with an N₂ stream. The slide was then incubated in a 0.1 mM solution of fluorescein in PBS buffer for 15 min, followed by rinsing sequentially with PBS buffer and Milli-Q water. After the slide was dried with an N₂ stream, the slide was imaged.

4.2.6. Imaging of a Photopatterned Slide

Patterned slides were imaged using the fluorescence microscope equipped with a pco.edge 4.2LT monochrome CMOS camera (PCO, Germany) and using a 10 \times /0.30 UPlanFL N objective. Fluorescent images were collected with an exposure of 2000 ms per frame, 4 frames per image, in a sequence of 25 images, equaling a total of 200 s. Each sequence was averaged in MATLAB and then shaded using the "levels" tool in the GIMP photoediting software. Slides photopatterned with 3-ethynyl perylene were excited at 405 nm using a filter cube containing an AT405/30x excitation filter (Chroma), a dichroic

mirror with a cutoff wavelength of 450 nm (Edmund Optics), and a 475/42 nm emission filter (Semrock) or a cube containing the same excitation filter but a dichroic mirror with a cutoff of 435 nm (Edmund Optics) and a 448/25 nm emission filter (Edmund Optics). Slides photopatterned with (1) FAM alkyne, 5-isomer; (2) fluorescein-labeled avidin; or (3) PEG stained with fluorescein were excited at 455 nm using a filter cube containing a 451/106 nm excitation filter, a dichroic mirror with a cutoff wavelength of 510 nm, and a 534/30 nm emission filter, all from Semrock.

Supporting Information

The Supporting Information is available free of charge at <https://pubs.acs.org/doi/10.1021/acsami.2c06946>.

- Experimental conditions used while testing silanization with MPS; results from the optimization of solvent and incubation time in 5 mM MPS; images from different postsilanization procedures using a standard 5 mM MPS in toluene for 24 h; UV–vis absorbance and fluorescence spectra of the two dyes; pattern used for determining the relationship between dose and subsequent fluorescence intensity; intensities from the first 10 min of the exposure tests for FAM on MPTMS; additional images; demonstration of observed bleaching for photopatterned FAM on a surface treated with MPS; synthesis procedure for MPS and related ^1H NMR spectra; original artwork; and explanation of provided MATLAB scripts for use in correcting the vignetting effect in our optical setup (PDF)
- MATLAB scripts used for the production of field corrections, image slice generation, and the automated processing of image sequences (ZIP)

Notes

The authors declare no competing financial interest.

Acknowledgments

The authors thank Dolev Rimmerman for his expertise in designing, assembling, testing, and training the authors on the operation of the inverted fluorescence microscope used in this research.

References

- 1 Hynes, M. J.; Maurer, J. A. Lighting the Path: Photopatternable Substrates for Biological Applications. *Mol. BioSyst.* **2013**, *9* (4), 559– 564, DOI: 10.1039/C2MB25403D
- 2 Kourtí, D.; Kanioura, A.; Chatzichristidi, M.; Beltsios, K. G.; Kakabakos, S. E.; Petrou, P. S. Photopatternable Materials for Guided Cell Adhesion and Growth. *Eur. Polym. J.* **2022**, *162* (October 2021), 110896, DOI: 10.1016/j.eurpolymj.2021.110896
- 3 Fruncillo, S.; Su, X.; Liu, H.; Wong, L. S. Lithographic Processes for the Scalable Fabrication of Micro- and Nanostructures for Biochips and Biosensors. *ACS Sens.* **2021**, *6* (6), 2002– 2024, DOI: 10.1021/acssensors.0c02704
- 4 Arrabito, G.; Gulli, D.; Alfano, C.; Pignataro, B. Writing Biochips[™]: High-Resolution Droplet-to-Droplet Manufacturing of Analytical Platforms. *Analyt.* **2022**, *147* (7), 1294– 1312, DOI: 10.1039/D1AN02295D

- 5 Delamarche, E.; Pereiro, I.; Kashyap, A.; Kaigala, G. V. Biopatterning: The Art of Patterning Biomolecules on Surfaces. *Langmuir* **2021**, *37* (32), 9637– 9651, DOI: 10.1021/acs.langmuir.1c00867
- 6 Liu, X.; Carbonell, C.; Braunschweig, A. B. Towards Scanning Probe Lithography-Based 4D Nanoprinting by Advancing Surface Chemistry, Nanopatterning Strategies, and Characterization Protocols. *Chem. Soc. Rev.* **2016**, *45* (22), 6289– 6310, DOI: 10.1039/C6CS00349D
- 7 Tauk, L.; Schröder, A. P.; Decher, G.; Giuseppone, N. Hierarchical Functional Gradients of PH-Responsive Self-Assembled Monolayers Using Dynamic Covalent Chemistry on Surfaces. *Nat. Chem.* **2009**, *1* (8), 649– 656, DOI: 10.1038/nchem.400
- 8 Myers, B. D.; Lin, Q. Y.; Wu, H.; Luijten, E.; Mirkin, C. A.; Dravid, V. P. Size-Selective Nanoparticle Assembly on Substrates by DNA Density Patterning. *ACS Nano* **2016**, *10* (6), 5679– 5686, DOI: 10.1021/acsnano.6b02246
- 9 Rolli, C. G.; Nakayama, H.; Yamaguchi, K.; Spatz, J. P.; Kemkemer, R.; Nakanishi, J. Switchable Adhesive Substrates: Revealing Geometry Dependence in Collective Cell Behavior. *Biomaterials* **2012**, *33* (8), 2409– 2418, DOI: 10.1016/j.biomaterials.2011.12.012
- 10 Weydert, S.; Girardin, S.; Cui, X.; Zürcher, S.; Peter, T.; Wirz, R.; Sterner, O.; Stauffer, F.; Aebersold, M. J.; Tanner, S.; Thompson-Steckel, G.; Forró, C.; Tosatti, S.; Vörös, J. A Versatile Protein and Cell Patterning Method Suitable for Long-Term Neural Cultures. *Langmuir* **2019**, *35* (8), 2966– 2975, DOI: 10.1021/acs.langmuir.8b03730
- 11 Xiong, M.; Gu, B.; Zhang, J.-D.; Xu, J.-J.; Chen, H.-Y.; Zhong, H. Glucose Microfluidic Biosensors Based on Reversible Enzyme Immobilization on Photopatterned Stimuli-Responsive Polymer. *Biosens. Bioelectron.* **2013**, *50*, 229– 234, DOI: 10.1016/j.bios.2013.06.030
- 12 Moser, I. Biosensor Arrays for Simultaneous Measurement of Glucose, Lactate, Glutamate, and Glutamine. *Biosens. Bioelectron.* **2002**, *17* (4), 297– 302, DOI: 10.1016/S0956-5663(01)00298-6
- 13 Schlereth, D. D. *Comprehensive Analytical Chemistry*; Elsevier, 2005; Vol. 44, Chapter 1, pp 1– 63 DOI: 10.1016/S0166-526X(05)44001-5 .
- 14 Liu, X.; Wang, H.; Herron, J. N.; Prestwich, G. D. Photopatterning of Antibodies on Biosensors. *Bioconjugate Chem.* **2000**, *11* (6), 755– 761, DOI: 10.1021/bc000006d
- 15 Jung, Y. K.; Jung, C.; Park, H. G. Photopatterned Polydiacetylene Images Using a DNA Bio-Photomask. *ACS Appl. Mater. Interfaces* **2016**, *8* (24), 15684– 15690, DOI: 10.1021/acsami.6b01830
- 16 Chittock, R. S.; Cooper, J.; Wharton, C. W.; Berovic, N.; Parkinson, N. S.; Jackson, J. B.; Beynon, T. D. Micrometre-Scale Bioluminescent Enzyme Photopatterning for Bioelectronics Applications. *Seventh Int. Conf. Organ. Mol. Films* **1996**, *284–285*, 776– 779, DOI: 10.1016/S0040-6090(95)08444-4
- 17 Oh, S. Y.; Jie, H. S.; Choi, H. S.; Choi, J. W. Deep UV Photopatterning of Self-Assembled Monolayer and Its Application in Bioelectronic Device. *AsiaNano 2002*; Tokyo, Japan, 2002; pp 237– 242.
- 18 Kaneko, S.; Yamaguchi, K.; Nakanishi, J. Dynamic Substrate Based on Photocleavable Poly(Ethylene Glycol): Zeta Potential Determines the Capability of Geometrical Cell Confinement. *Langmuir* **2013**, *29* (24), 7300– 7308, DOI: 10.1021/la304569e
- 19 Luo, W.; Yousaf, M. N. Tissue Morphing Control on Dynamic Gradient Surfaces. *J. Am. Chem. Soc.* **2011**, *133* (28), 10780– 10783, DOI: 10.1021/ja204893w
- 20 Mosiewicz, K. A.; Kolb, L.; Van Der Vlies, A. J.; Martino, M. M.; Lienemann, P. S.; Hubbell, J. A.; Ehrbar, M.; Lutolf, M. P. In Situ Cell Manipulation through Enzymatic Hydrogel Photopatterning. *Nat. Mater.* **2013**, *12* (11), 1072– 1078, DOI: 10.1038/nmat3766
- 21 Sun, Q.; Wang, D.; Li, Y.; Zhang, J.; Ye, S.; Cui, J.; Chen, L.; Wang, Z.; Butt, H.-J.; Vollmer, D.; Deng, X. Surface Charge Printing for Programmed Droplet Transport. *Nat. Mater.* **2019**, *18* (9), 936– 941, DOI: 10.1038/s41563-019-0440-2

- 22** Sekeroglu, K.; Gurkan, U. A.; Demirci, U.; Demirel, M. C. Transport of a Soft Cargo on a Nanoscale Ratchet. *Appl. Phys. Lett.* **2011**, *99* (6), 063703– 063703, DOI: 10.1063/1.3625430
- 23** Chen, C.; Xu, P.; Li, X. Regioselective Patterning of Multiple SAMs and Applications in Surface-Guided Smart Microfluidics. *ACS Appl. Mater. Interfaces* **2014**, *6* (24), 21961– 21969, DOI: 10.1021/am508120s
- 24** Nicosia, C.; Huskens, J. Reactive Self-Assembled Monolayers: From Surface Functionalization to Gradient Formation. *Mater. Horiz.* **2014**, *1* (1), 32– 45, DOI: 10.1039/C3MH00046J
- 25** Zhang, X.; Zhang, M.; Wu, M.; Yang, L.; Liu, R.; Zhang, R.; Zhao, T.; Song, C.; Liu, G.; Zhu, Q. Photoresponsive Bridged Polysilsesquioxanes for Protein Immobilization/Controlled Release and Micropatterns. *ACS Appl. Mater. Interfaces* **2021**, *13* (30), 36370– 36379, DOI: 10.1021/acsami.1c10542
- 26** Jonkheijm, P.; Weinrich, D.; Köhn, M.; Engelkamp, H.; Christianen, P. C. M.; Kuhlmann, J.; Maan, J. C.; Nüsse, D.; Schroeder, H.; Wacker, R.; Breinbauer, R.; Niemeyer, C. M.; Waldmann, H. Photochemical Surface Patterning by the Thiol-Ene Reaction. *Angew. Chem., Int. Ed.* **2008**, *47* (23), 4421– 4424, DOI: 10.1002/anie.200800101
- 27** Dadfar, S. M. M.; Sekula-Neuner, S.; Bog, U.; Trouillet, V.; Hirtz, M. Site-Specific Surface Functionalization via Microchannel Cantilever Spotting (MCS): Comparison between Azide-Alkyne and Thiol-Alkyne Click Chemistry Reactions. *Small* **2018**, *14* (21), 1800131, DOI: 10.1002/smll.201800131
- 28** Piner, R. D.; Zhu, J.; Xu, F.; Hong, S.; Mirkin, C. A. Dip-Pen” Nanolithography. *Science* **1999**, *283* (5402), 661– 663, DOI: 10.1126/science.283.5402.661
- 29** Liu, G.; Hirtz, M.; Fuchs, H.; Zheng, Z. Development of Dip-Pen Nanolithography (DPN) and Its Derivatives. *Small* **2019**, *15* (21), 1900564, DOI: 10.1002/smll.201900564
- 30** Huo, F.; Zheng, G.; Liao, X.; Giam, L. R.; Chai, J.; Chen, X.; Shim, W.; Mirkin, C. A. Beam Pen Lithography. *Nat. Nanotechnol.* **2010**, *5* (9), 637– 640, DOI: 10.1038/nnano.2010.161
- 31** Zhou, Y.; Xie, Z.; Brown, K. A.; Park, D. J.; Zhou, X.; Chen, P.-C.; Hirtz, M.; Lin, Q.-Y.; Dravid, V. P.; Schatz, G. C.; Zheng, Z.; Mirkin, C. A. Apertureless Cantilever-Free Pen Arrays for Scanning Photochemical Printing. *Small* **2015**, *11* (8), 913– 918, DOI: 10.1002/smll.201402195
- 32** Bian, S.; Zieba, S. B.; Morris, W.; Han, X.; Richter, D. C.; Brown, K. A.; Mirkin, C. A.; Braunschweig, A. B. Beam Pen Lithography as a New Tool for Spatially Controlled Photochemistry, and Its Utilization in the Synthesis of Multivalent Glycan Arrays. *Chem. Sci.* **2014**, *5* (5), 2023– 2030, DOI: 10.1039/c3sc53315h
- 33** Valles, D. J.; Zholdassov, Y. S.; Braunschweig, A. B. Evolution and Applications of Polymer Brush Hypersurface Photolithography. *Polym. Chem.* **2021**, *12* (40), 5724– 5746, DOI: 10.1039/D1PY01073E
- 34** Perl, A.; Reinhoudt, D. N.; Huskens, J. Microcontact Printing: Limitations and Achievements. *Adv. Mater.* **2009**, *21* (22), 2257– 2268, DOI: 10.1002/adma.200801864
- 35** Escorihuela, J.; Bañuls, M. J.; Puchades, R.; Maquieira, Á. DNA Microarrays on Silicon Surfaces through Thiol-Ene Chemistry. *Chem. Commun.* **2012**, *48* (15), 2116– 2118, DOI: 10.1039/c2cc17321b
- 36** Martin, T. A.; Herman, C. T.; Limpoco, F. T.; Michael, M. C.; Potts, G. K.; Bailey, R. C. Quantitative Photochemical Immobilization of Biomolecules on Planar and Corrugated Substrates: A Versatile Strategy for Creating Functional Biointerfaces. *ACS Appl. Mater. Interfaces* **2011**, *3* (9), 3762– 3771, DOI: 10.1021/am2009597
- 37** Zhou, S.; Metcalf, K. J.; Bugga, P.; Grant, J.; Mrksich, M. Photoactivatable Reaction for Covalent Nanoscale Patterning of Multiple Proteins. *ACS Appl. Mater. Interfaces* **2018**, *10* (47), 40452– 40459, DOI: 10.1021/acsami.8b16736

- 38** Fiddes, L. K.; Chan, H. K. C.; Lau, B.; Kumacheva, E.; Wheeler, A. R. Durable, Region-Specific Protein Patterning in Microfluidic Channels. *Biomaterials* **2010**, *31* (2), 315– 320, DOI: 10.1016/j.biomaterials.2009.09.040
- 39** Waldbaur, A.; Waterkotte, B.; Schmitz, K.; Rapp, B. E. Maskless Projection Lithography for the Fast and Flexible Generation of Grayscale Protein Patterns. *Small* **2012**, *8* (10), 1570– 1578, DOI: 10.1002/smll.201102163
- 40** Strale, P.-O.; Azoune, A.; Bugnicourt, G.; Lecomte, Y.; Chahid, M.; Studer, V. Multiprotein Printing by Light-Induced Molecular Adsorption. *Adv. Mater.* **2016**, *28* (10), 2024– 2029, DOI: 10.1002/adma.201504154
- 41** Carbonell, C.; Valles, D.; Wong, A. M.; Carlini, A. S.; Touve, M. A.; Korpanty, J.; Gianneschi, N. C.; Braunschweig, A. B. Polymer Brush Hypersurface Photolithography. *Nat. Commun.* **2020**, *11* (1), 1244, DOI: 10.1038/s41467-020-14990-x
- 42** Hoyle, C. E.; Bowman, C. N. Thiol-Ene Click Chemistry. *Angew. Chem., Int. Ed.* **2010**, *49* (9), 1540– 1573, DOI: 10.1002/anie.200903924
- 43** Feng, W.; Li, L.; Ueda, E.; Li, J.; Heißler, S.; Welle, A.; Trapp, O.; Levkin, P. A. Surface Patterning via Thiol-Yne Click Chemistry: An Extremely Fast and Versatile Approach to Superhydrophilic-Superhydrophobic Micropatterns. *Adv. Mater. Interfaces* **2014**, *1* (7), 1400269, DOI: 10.1002/admi.201400269
- 44** Walker, D.; Singh, D. P.; Fischer, P. Capture of 2D Microparticle Arrays via a UV-Triggered Thiol-Yne “Click” Reaction. *Adv. Mater.* **2016**, *28* (44), 9846– 9850, DOI: 10.1002/adma.201603586
- 45** DeForest, C. A.; Polizzotti, B. D.; Anseth, K. S. Sequential Click Reactions for Synthesizing and Patterning Three-Dimensional Cell Microenvironments. *Nat. Mater.* **2009**, *8* (8), 659– 664, DOI: 10.1038/nmat2473
- 46** Buhl, M.; Vonhören, B.; Ravoo, B. J. Immobilization of Enzymes via Microcontact Printing and Thiol-Ene Click Chemistry. *Bioconjugate Chem.* **2015**, *26* (6), 1017– 1020, DOI: 10.1021/acs.bioconjchem.5b00282
- 47** Wendeln, C.; Rinnen, S.; Schulz, C.; Arlinghaus, H. F.; Ravoo, B. J. Photochemical Microcontact Printing by Thiol-Ene and Thiol-Yne Click Chemistry. *Langmuir* **2010**, *26* (20), 15966– 15971, DOI: 10.1021/la102966j
- 48** Lee, T.-J.; Chau, L.-K.; Huang, C.-J. Controlled Silanization: High Molecular Regularity of Functional Thiol Groups on Siloxane Coatings. *Langmuir* **2020**, *36* (21), 5935– 5943, DOI: 10.1021/acs.langmuir.0c00745
- 49** Yaakov, N.; Chaikin, Y.; Wexselblatt, E.; Tor, Y.; Vaskevich, A.; Rubinstein, I. Application of Surface Click Reactions to Localized Surface Plasmon Resonance (LSPR) Biosensing. *Chem. – Eur. J.* **2017**, *23* (42), 10148– 10155, DOI: 10.1002/chem.201701511
- 50** Chen, J.-J.; Struk, K. N.; Brennan, A. B. Surface Modification of Silicate Glass Using 3-(Mercaptopropyl)Trimethoxysilane for Thiol-Ene Polymerization. *Langmuir* **2011**, *27* (22), 13754– 13761, DOI: 10.1021/la202225g
- 51** Cras, J. J.; Rowe-Taitt, C. A.; Nivens, D. A.; Ligler, F. S. Comparison of Chemical Cleaning Methods of Glass in Preparation for Silanization. *Biosens. Bioelectron.* **1999**, *14* (8–9), 683– 688, DOI: 10.1016/S0956-5663(99)00043-3
- 52** Vistas, C. R.; Águas, A. C. P.; Ferreira, G. N. M. Silanization of Glass Chips—A Factorial Approach for Optimization. *Appl. Surf. Sci.* **2013**, *286*, 314– 318, DOI: 10.1016/j.apsusc.2013.09.077
- 53** Lakowicz, J. R.; Malicka, J.; D’Auria, S.; Gryczynski, I. Release of the Self-Quenching of Fluorescence near Silver Metallic Surfaces. *Anal. Biochem.* **2003**, *320* (1), 13– 20, DOI: 10.1016/S0003-2697(03)00351-8
- 54** McConnell, D. B. Biotin’s Lessons in Drug Design. *J. Med. Chem.* **2021**, *64* (22), 16319– 16327, DOI: 10.1021/acs.jmedchem.1c00975

- 55 Chen, S.; Smith, L. M. Photopatterned Thiol Surfaces for Biomolecule Immobilization. *Langmuir* **2009**, *25* (20), 12275– 12282, DOI: 10.1021/la9017135
- 56 Holden, M. A.; Jung, S.-Y.; Cremer, P. S. Patterning Enzymes Inside Microfluidic Channels via Photoattachment Chemistry. *Anal. Chem.* **2004**, *76* (7), 1838– 1843, DOI: 10.1021/ac035234q
- 57 Shuster, M. J.; Vaish, A.; Cao, H. H.; Guttentag, A. I.; McManigle, J. E.; Gibb, A. L.; Martinez, M. M.; Nezarati, R. M.; Hinds, J. M.; Liao, W. S.; Weiss, P. S.; Andrews, A. M. Patterning Small-Molecule Biocapture Surfaces: Microcontact Insertion Printing vs. Photolithography. *Chem. Commun.* **2011**, *47* (38), 10641– 10643, DOI: 10.1039/c1cc13002a
- 58 Mela, P.; Onclin, S.; Goedbloed, M. H.; Levi, S.; García-Parajó, M. F.; van Hulst, N. F.; Ravoo, B. J.; Reinhoudt, D. N.; van den Berg, A. Monolayer-Functionalized Microfluidics Devices for Optical Sensing of Acidity. *Lab Chip* **2005**, *5* (2), 163– 170, DOI: 10.1039/B409978H
- 59 Nicosia, C.; Krabbenborg, S. O.; Reinhoudt, D. N.; Huskens, J. In Situ Fluorimetric Detection of Micrometer-Scale PH Gradients at the Solid/Liquid Interface. *Supramol. Chem.* **2013**, *25* (9–11), 756– 766, DOI: 10.1080/10610278.2013.814775
- 60 Singh, G.; Rani, S.; Arora, A.; Aulakh, D.; Wriedt, M. Thioester-Appended Organosilatrane: Synthetic Investigations and Application in the Modification of Magnetic Silica Surfaces. *New J. Chem.* **2016**, *40* (7), 6200– 6213, DOI: 10.1039/C6NJ00011H
- 61 Zhu, M.; Lerum, M. Z.; Chen, W. How To Prepare Reproducible, Homogeneous, and Hydrolytically Stable Aminosilane-Derived Layers on Silica. *Langmuir* **2012**, *28* (1), 416– 423, DOI: 10.1021/la203638g
- 62 Edelstein, A. D.; Tsuchida, M. A.; Amodaj, N.; Pinkard, H.; Vale, R. D.; Stuurman, N. Advanced Methods of Microscope Control Using MManager Software. *J. Biol. Methods* **2014**, *1* (2), e10, DOI: 10.14440/jbm.2014.36